Protostellar Outflow-Driven Turbulence: A Numerical Look

Michael Gorelick

Abstract

Protostellar outflows play an essential role in the morphology of molecular clouds. By driving supersonic turbulence, the outflows help sustain the cloud's stability by providing an effective pressure which also serves to slow down star formation rates. This paper presents numerical data supporting the model presented by Matzner (2007) characterizing supersonic turbulence driven by both spherical and collimated regions of finite impulse. Using an rTVD hydrodynamic solver we conduct careful numerical experiments to test the predictions that a) the collimated case results in stronger turbulent line widths b) characteristic lengths and times are increased in the collimated regime and c) the velocity dispersion displays features at the characteristic scales d) the energy spectrum follows Burger turbulence. We find great agreement on all points except point (d) where we find a steepening for large k. Furthermore, we provide an empirical connection between the the coupling to the gas of the spherical and collimates outflows.

1. Introduction

Star formation rates have been observed to be slower than previously thought. Classically star formation happens when gravity pulls gas into very high density regions. As such we should expect this to work with a free-fall time, $t_{ff} = \sqrt{\frac{3\pi}{32G\rho}}$, resulting in mass being converted to stars at a rate of $\dot{M}_* = SFR_{ff}\frac{M_{gas}}{t_{ff}}$ with a star formation rate normalized to the free fall time of $SFR_{ff} \sim 1$. However, observation has constantly shown that star formation rates occur at a much slower rate. Krumholz and Tan (2007) show a star formation rate in very dense regions of $SFR_{ff} \sim 10^{-1.7}$ and Zuckerman and Palmer (1974) indicated a rate of only a few percent from a sample of 20 giant molecular clouds. Even planetary orbital stability seems to indicate that the solar system was born in a relatively sparsely inhabited cluster with only 10^3 inhabitance (Adams and Laughlin 2001) which would seem to indicate a lowered star formation rate in that region. Turbulence also helps solve a problem of molecular cloud stability, if they are not simply transient features, and the observation that MC's are quite diffuse, even in the face of great self-gravity, resulting in the loss of more mass than is transformed into stars. Without some sort of pseudo-pressure the entire cloud should collapse in about a free-fall time however virial analysis shows that turbulence is sufficient for stability – even more-so with the addition of magnetic fields.

A substantial problem with this turbulence is the origin of the driving. Some theories explain that the molecular cloud originates from instabilities in galactic spiral arms and those instabilities result in the required turbulence down to the dense protocluster regions, however simulations have shown that supersonic turbulence decays in the order of a few free-fall times (Stone et al. 1998; Low 1999). In giant molecular clouds ($R \sim 10pc,\ M \sim 10^5 - 10^6 M_\odot,\ n \sim 100\frac{1}{cm^3}$ resulting in $t_{ff} \sim 4.3Myr$) inflating HII regions from large O or B type stars and supernovae can be seen as a driving source, however this falls short for denser and more compact regions ($R \sim 1pc,\ M \sim 10^3 M_\odot,\ n \sim 10^4\frac{1}{cm^3}$ resulting in $t_{ff} \sim 0.43Myr$) where much faster time-scales are required. One possible source for replenishing the turbulent energy is protostellar outflows.

Protostellar outflows have the benefit of injecting orders of magnitudes more momentum than photo-ionization from HII regions while being more frequent than supernovae. In fact, protostellar outflows and star formation seem to be ubiquitous since the outflows are launched in the

early phases of stellar evolution (as opposed to HII regions which require O or B type stars), and it seems to be a phase that all stars go through. With protostellar outflow-driven turbulence we have stars being created from density enhancements due to any original background turbulence in the cloud. These newly formed stars launch jets with typical velocity on the order of $100\frac{km}{s}$. These stars become a source of turbulence; new stars are essentially maintaining stability in their cloud while inhibiting excessive formation. The typical turbulent velocities of star cluster forming regions is around $1-2\frac{km}{s}$ so outflows are significant even if their shocks are radiative and only a small fraction of the cloud's mass is swept up by the wind. This evolution from background dominated to a outflow dominated turbulence is explored in Nakamura and Li (2007) through an MHD simulation whose results fit quite well to observations of NGC1333. See McKee and Ostriker (2007) for an overview of the macroscopic effects of turbulent star formation.

Matzner (2007) uses dimensional analysis to estimate the properties of supersonic turbulence driven by spherical explosions. He then speculates about the changes in dynamics if the driving was changed from spherical to collimated. This model predicts that the turbulence will be enhanced and characteristic length and time scales will be increased in the collimated case in addition to properties of the velocity dispersion and power spectrum at these characteristic scales. This project aims to test these predictions with carefully controlled numerical experiments which allow us to provide detailed dynamical information on supersonic outflow-driven turbulence.

2. Model

We begin by considering a volume with constant density ρ_0 and a zero velocity field whose turbulence is driven from spherical impulses of strength $\mathcal{I}$ that occur at a rate per unit volume of $\mathcal{S}$. The event of injecting an impulse into the medium launches an expanding shell which should merge with others at some characteristic time and length scale. Matzner (2007) uses dimensional analysis to estimate these scales and finds

$$m = \left(\frac{\rho_0^4\mathcal{I}^2}{\mathcal{S}^2}\right)^{1/7}, \ell_{merge} = \left(\frac{\mathcal{I}}{\rho_0\mathcal{S}}\right)^{1/7}, \quad (1)$$

$$t_{merge} = \left(\frac{\rho_0^3}{\mathcal{I}^3\mathcal{S}^4}\right)^{1/7}, \quad (2)$$

which defines a characteristic mass, a merging length scale and a merging time scale. We would expect the volume to reach steady state at about $t \lesssim t_{merge}$ when the spherical impulses start to merge and the space becomes filled with the added momenta. Of particular interest is a quantity defining the characteristic velocity of the impulses at the merging length

$$v_{merge} = \frac{\ell_{merge}}{t_{merge}} = \left(\frac{\mathcal{I}^4\mathcal{S}^3}{\rho_0^4}\right)^{1/7}. \quad (3)$$

This analysis outlines an idealized model of outflow driven turbulence by spherical and impulsive outflows. Looking at NGC1333 and estimating $\mathcal{I} = 10^{39.6} g\,cm\,s^{-1}$, $\mathcal{S} = 10^{-67.2} cm^{-3}\,s^{-1}$ and $\rho_0 = 10^{-19.6} g\,cm^{-3}$ we find that $\ell_{merge} = 0.38pc$, $t = 0.34Myr$, $m = 19M_\odot$, and $\ell/t = 1.1km\,s^{-1}$. We must note that the dimensions of the mass, length and time do not enter the numerical simulation. The important quantities in that context are: the Mach number $\frac{\sigma}{c_s}$ at the saturation state, the ratio of merging scale, ℓ_{merge}, to the box size, L_{box}, and finally the ratio of the merging scale to the injection radius. Of these quantities, only the Mach number represents any physical significance (although Matzner (2007) argues that it isn't significant to the dynamics of the turbulence) while the others provide numerical parameters.

Matzner goes on to estimate the efficiency of these outflows by defining a coupling factor, Λ, which quantifies how well the pseudo pressure over the merging scale per unit mass, due to the outflows correlates to bulk motion of the gas. This can be stated in terms of an approximation to the one-dimensional velocity dispersion, $\sigma(r)$, at the merging scale by

$$\sigma(\ell_{merge})^2 = \Lambda^2\frac{\mathcal{S}\mathcal{I}}{\rho_0}\ell_{merge}. \quad (4)$$

To make this model more physical the question of collimation is addressed to include the effects of

bipolar jets. We use a model for the impulse of a bipolar protostellar jets launched by x-winds,

$$\hat{\mathcal{I}}(\phi) = \mathcal{I}P(\phi),\ P(\theta) = \mathcal{X}(\theta_0) \cdot \frac{1}{1+\theta_0^2 - cos(\phi)^2}, \tag{5}$$

where θ_0 is the opening angle (such that $P(\phi) = 1\ \forall\ \phi$ when $\theta_0 = \infty$), ϕ is the angle from the axis of the jet, and $\mathcal{X}(\theta_0)$ is such that $\int^V \hat{\mathcal{I}} dV = \mathcal{I}$ so that the total injected momentum remains the same as the spherical case (Matzner and McKee, 1999). This relationship is used to add an angular dependence to the the local injected momentum. We require, however, that $\int_V P(\phi) dV = 1$ (where V is the outflow region) so that the total outflow momentum remains unaffected. A result of the collimation is that the quantities given in equations 1 and 3 no longer strictly apply due to the added angular dependence of $\mathcal{I}$. For example, with an estimate of the opening angle $\theta_0 \sim 10^{-2}$ from observed objects we find $\frac{v_{merge}(\theta=0)}{v_{merge}(\theta=\pi/2)} \sim 2 \cdot 10^2$.

In order to determine the effects of the collimation we choose to compare the resultant turbulent energies from collimated outflows versus spherical. To achieve this we define an enhancement factor,

$$\varepsilon = \left. \frac{\sigma^2_{\theta_0 \neq \infty}(\ell_{merge})}{\sigma^2_{\theta=\infty}(\ell_{merge})} \right|_{t \gg t_{merge}}, \tag{6}$$

in terms of the 1D velocity dispersion during steady state which can alternatively be seen as a ratio of effective turbulent pressures. Matzner (2007) predicts a value of $\varepsilon > 1$ due to the increased velocities injected into the medium due to collimation.

With these relations we intend to show a relationship between the collimated and spherical case. This correlation will allow the use of the analytical spherical model for physical objects whose turbulence is stirred by highly collimated beams. Furthermore, by characterizing the turbulence driven by collimated beams observational parameters, in the form of line widths, can be established. This will not only formulate an observational method for verification of the theories but will also create an analytical approach to inferring the turbulent properties inside a molecular cloud.

3. Numerics

We use a 2nd order rTVD code using an upwind scheme as described by Pen et al. (2003). rTVD is a relaxing total variation diminishing method used to solve for the evolution of conserved quantities while preventing numerical instabilities (Jin and Xin 1995). This allows us to strictly conserve mass and momentum and allows us to utilize a strictly isothermal grid. The isothermal condition is a standard feature of molecular cloud studies since it accounts for the large densities and molecular nature of the gas (allowing it to readily radiate and relax to a low temperature) and because gas pressure is not important for supersonic motions. With these tools a hydrodynamic and periodic grid is created in simulation units such that the grid width, sound speed and initial density are normalized to unity ($dx = c_s = \rho_0 = 1$). The grid was chosen to be 400^3 cells large and have CFL=0.95. The CLF number defines the courant condition which allows us to set the time-steps such that no motion can go more than a specified distance. Our restriction on the CFL number guarantees that the time steps are chosen such that no motion can move more than $0.95dx$ in one time step to insure stability.

To further guarantee stability, the freezing number which relaxes the flux of conserved quanta-ties through cell walls was chosen to be constant inside the grid (See Jin and Xin 1995). This issue was explored with an experiment consisting of multiple runs with similar parameters however some had locally calculated freezing speed ($c = c_s + |\vec{v}|$ where v is the velocity field) and others simply maintained the maximum value ($c = max\{c_s + |\vec{v}|\}$ over the entire grid). It was found that a locally calculated freezing speed performed well for "tame" gas however once the expanding shells merged instabilities were formed. These instabilities were in the form of negative densities caused by the freezing speed not sufficiently limiting the flux through grid cells and essentially over evacuating regions. With a globally calculated freezing speed these instabilities did not present themselves. Both version did, however yield the same line widths and kinetic energies during the stable period. We also should note that due to the nature of the supersonic turbulence and the use of Strang splitting that

the time-step would periodically be insufficiently small during the second Strang sweep and thus violate the courant condition. When this effect is taking into account and with the use of a constant freezing speed we achieve a perfectly stable computational grid.

During the run, the grid is analyzed and outflows are randomly placed as given by the Poisson distribution with the expected number of events $\lambda = L_{box}^3 \cdot \mathcal{S} \cdot dt$. At each location a radius of $r_{inj} \ll \ell_{merge}$ is initialized given the collimation profile of the run. In order to avoid un-physically large velocities due to momentum injection in low density regions a density of

$$P(|\phi|) \cdot \frac{3\mathcal{I}}{4\pi r_{inj}^3 v_{max}} \cdot dx$$

is added to every grid cell where $P(|\phi|)$ is given by equation (5). To ensure that mass is still conserved and to protect the bulk dynamics the we multiply the state matrix (density and 3-momentum) by $\frac{M_{tot}}{M_{tot}+dM}$ before the rTVD step. This method also ensures greater homogeneity of injected momenta as compared to other methods, such as simply allowing the additional mass to remain in the grid or limiting the momentum injected into local regions based on a cutoff velocity. The dynamics of the grid remain unchanged before and after this step since the accelerations remain invariant to this density scaling.

In order to test the accuracy of the data, a simplified numerical study was done where two runs were initiated with the same parameters but different resolutions (Runs I and VI in Table 4). The 3D velocity dispersions seen in Figure 5 show similar dynamics in both however Run I has more stable velocities. This can be seen as a statistical feature to do the larger sampling set gained by the larger grid. Both runs, however, reach a saturation 3D velocity dispersion of $v_{rms}^2 \approx 9$ which yielded similar coupling coefficients (see Figure 4). This trend can be seen even though, due to time constraints, Run I was not in the steady state for an extended time. To further validate this conclusion, more trials can be done at varying box sizes and resolutions while holding all physical parameters constant. If let run well into the steady state the respective values for calculated quantities, the coupling coefficients for example, could be compared and an infinite resolution result can be interpolated (a method known as Richardson Interpolation).

4. Results

In order to test the turbulence driven by outflows and find a correlation between the spherical and collimated jets, runs were conduced as given by Table 4. The values of $\mathcal{I}$ and $\mathcal{S}$ were chosen to maximize $\frac{\ell_{merge}}{L_{box}}$ while maintaining a sufficiently supersonic merging velocity typical of protostellar outflows.

Visual inspection of density slices in Figure 5 show qualitative differences between the two extreme cases of collimation. Of particular interest is the variation of morphology of outflow fossil cavities (Cunningham et al. 2008) which qualitatively indicates the effects of collimation on the resultant turbulence. These features have been observed in NGC1333 (Quillen et al. 2005) with mean velocities $v_{fossil} \approx 1.6 - 3.3c_s$.

Furthermore, spherical outflows seem to merge more quickly because of the symmetric nature of the injection, collimated outflows augmented velocities at the beams more than make up for this. We can say that spherical outflows start merging with velocities near v_{merge} however this claim cannot be used for bipolar jets. However, for parameters like those for run III and $\phi = 0$ the beam can travel $\sim 5.5 \cdot \ell_{merge}$ before slowing down to this velocity. This is a valid argument because we are using the isothermal case and thus line widths only include contributions from kinetic energies.

Run	θ_0	t_{merge}	λ^2
I	∞	$8\sqrt{\frac{c_s}{dx}}$	0.49
II	0.5	$8\sqrt{\frac{c_s}{dx}}$	0.64
III	0.05	$8\sqrt{\frac{c_s}{dx}}$	0.84
IV	∞	$10\sqrt{\frac{c_s}{dx}}$	0.54
V	0.5	$10\sqrt{\frac{c_s}{dx}}$	0.81
VI	∞	$8\sqrt{\frac{c_s}{dx}}$	0.48

Table 2: Coupling coefficient (λ^2) for various cases of collimation (θ_0) and merging times (t_{merge}).

The morphological differences caused by collimation can be seen in the root mean squared velocities and, from the one-dimensional line widths, coupling coefficients (Figures 5 and 4 respectively). We immediately see that higher colli-

Run #	$\mathcal{I}$	$\mathcal{S}$	θ_0	l_{merge}	v_{char}	t_{merge}	L_{box}
I	20000	$1.5625 \cdot 10^{-5}$	∞	$8dx$	$2.5c_s$	$8\sqrt{\frac{c_s}{dx}}$	$400dx$
II	20000	$1.5625 \cdot 10^{-5}$	0.5 (28°)	$8dx$	$2.5c_s$	$8\sqrt{\frac{c_s}{dx}}$	$400dx$
III	20000	$1.5625 \cdot 10^{-5}$	0.05(2.8°)	$8dx$	$2.5c_s$	$8\sqrt{\frac{c_s}{dx}}$	$400dx$
IV	16000	$1.25 \cdot 10^{-5}$	∞	$10dx$	$2.0c_s$	$10\sqrt{\frac{c_s}{dx}}$	$400dx$
V	16000	$1.25 \cdot 10^{-5}$	0.5(28°)	$10dx$	$2.0c_s$	$10\sqrt{\frac{c_s}{dx}}$	$400dx$
VI	20000	$1.5625 \cdot 10^{-5}$	∞	$8dx$	$2.5c_s$	$8\sqrt{\frac{c_s}{dx}}$	$200dx$

Table 1: Run Parameters

mated outflows have a greater propensity for coupling to the background gas with results from greater turbulent mixing velocities as evident in the saturation levels of v_{rms}. One important property to note is that the gas does not reach the steady state until $\sim 2 \cdot t_{merge}$ regardless of collimation when not only do the outflows merge but also fill all the space. This fits well with predictions given directly from combinations of v_{merge}, ℓ_{merge} and ρ_0.

The coupling coefficients can be used to calculate the enhancement factors for the collimated runs. The results in Figure 6 are in good agreement with those predicted in Matzner (2007). It is interesting to note the inverse proportionality ε to θ_0 and v_{merge}. This seems to be a result of greater gradients of momentum in the expanding shock and a longer time of expansion before merging resulting in more opportunity to advect momentum into the background.

Run	θ_0	v_{merge}	ε
II	0.5	$2.5c_s$	1.71
III	0.05	$2.5c_s$	2.94
V	0.5	$2.0c_s$	2.25

Table 3: Turbulent enhancement factor with respect to the spherical case for various cases of collimation (θ_0) and merging velocities (v_{merge}).

Applying a logarithmic fit to the calculated coupling coefficients of runs I, II, and III we find the expression for calculating λ^2 given the results of a similar spherical run and $\theta_0 < \infty$

$$\lambda^2_{col} \approx \mathcal{F}(\mathcal{I}, \mathcal{S}, \rho_0) \cdot \ln\left(\frac{1-\theta_0}{\theta_0}\right) + \lambda^2_{sph} \qquad (7)$$

$$\mathcal{F}(\mathcal{I}, \mathcal{S}, \rho_0) = \begin{cases} 0.11; \ Runs\ I/II/III \\ 0.25; \ Runs\ IV/V \end{cases} . \qquad (8)$$

Given the amounts of data used in the fit this expression should only be seen as rough estimate, however with more trials $\mathcal{F}$ can be found in an explicit form. It is interesting to note that this formulation, as expected, always yields a higher collimated coupling coefficient compared to the spherical case. In future work a comparison could be made with equation 27 from Matzner (2007) which states

$$\varepsilon = \frac{\int_0^{S_{tot}} r\mathcal{I} d\mathcal{S}}{\left[3\mathcal{I}^4\mathcal{S}^3/(4\pi\phi_m\Lambda\rho_0^{1/2})\right]^{2/7}}$$

where $\phi_m > 1$ if outflows are more prone to be formed in over-densities and $\mathcal{S}_{tot}$ is the total number of jet launchings.

Finally, we provide the energy spectrum of each run in order to characterize the type of turbulence. Figure 4 shows the energy spectrums at $t \gg t_{merge}$ for both the spherical and highly collimated case. Both scale approximately like $E(k) \sim k^{-\beta}$ with $\beta \sim 4$ for $k > \ell^{-1}_{merge}$ contrary to the prediction of $\beta \sim 2$ following from Burgers turbulence (Kida 1979). This could be a result of symmetry being added to the outflow injection because of the box's periodicity. This is supported by the observation that the spectrum for $k > \ell^{-1}_{merge}$ steepen with time. Alternatively, this can be seen as a result of expanding shells sweeping up small scale eddies. This would effectively reduce the energy in the small scale (high k) and produce this steepened spectrum (Carroll et al. 2009). On the other-hand, for $k \leq \ell^{-1}_{merge}$ we have a plateau in the spectral energy gives greater physical significance to ℓ_{merge} as the driving scale.

5. Summary

From our observation we see, in general, a very tight relationship to the predictions in Matzner

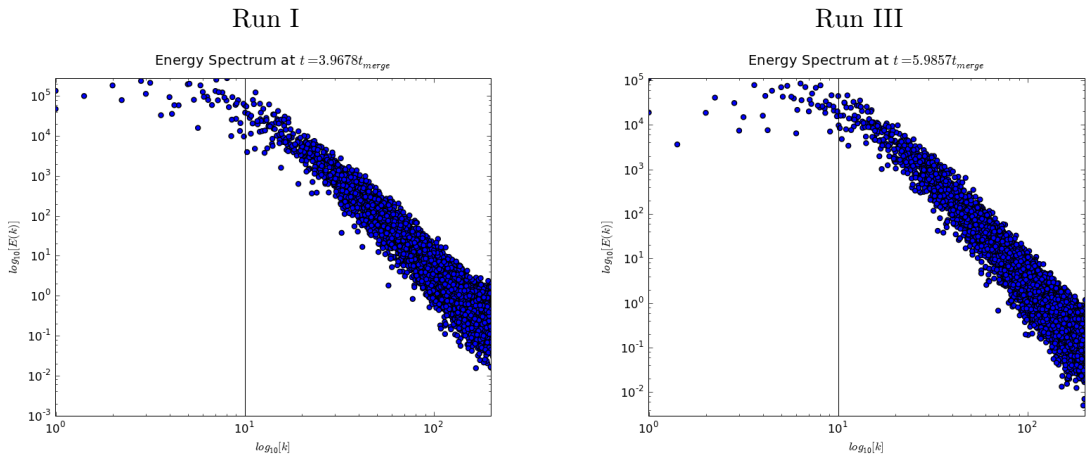

Fig. 1.— Energy spectrum at steady state for run I and III

(2007). As predicted there is an increase in the coupling coefficient and enhancement factors as well as the characteristic length and time scales due to collimation, in addition to characteristics in the velocity dispersion. We did, however, find a steepened energy spectrum of $\beta \sim 4$ rather than the expected $\beta \sim 2$. Furthermore we are able to take the numerical data to establish the connection between the idealized spherical to the collimated case. This is an important step in the model since protostellar outflows are characterized as very strongly bipolar. Furthermore, by treating the problem with pure hydrodynamics, we provide the ability to, with comparison to previous MHD simulations, segregate effects such as intrinsic stability of the molecular clouds due to entrained magnetic fields in order to greater dissect the problem.

In order to make our conclusion more accurate more trials must be done whose runtime will go well into $\sim 10 t_{merge}$. Most importantly this would include an explicit formulation of $\mathcal{F}$ (equation 8). Due to previous numerical problems this was not possible however we are now able to achieve long run-times with large grids. Other interesting features to inspect would be the effects of giving injection probability proportional to the local free-fall time and to vary outflow strength and collimation accordingly. This would enable us to inspect the model's aptitude at modeling more physical situations.

The author wishes to thank Christopher Matzner for all his support. It would not have been possible without the many discussions, explanations and words of encouragement.

REFERENCES

Fred C Adams and Gregory Laughlin. Constraints on the birth aggregate of the solar system. *Icarus*, 150:151, Mar 2001. doi: 10.1006/icar.2000.6567. URL `http://adsabs.harvard.edu/cgi-bin/nph-data_query?bibcode=2001Icar..150..151A&link_type=ABSTRACT`. (c) 2001: Academic Press.

Jonathan J Carroll, Adam Frank, Eric G Blackman, Andrew J Cunningham, and Alice C Quillen. Outflow-driven turbulence in molecular clouds. *The Astrophysical Journal*, 695:1376, Apr 2009. doi: 10.1088/0004-637X/695/2/1376. URL `http://adsabs.harvard.edu/cgi-bin/nph-data_query?bibcode=2009ApJ...695.1376C&link_type=ABSTRACT`.

Andrew J Cunningham, Adam Frank, Jonathan Carroll, Eric G Blackman, and Alice C Quillen. Protostellar outflow evolution in turbulent environments. *eprint arXiv*, 0804:4197, Apr 2008. URL `http://adsabs.harvard.edu/cgi-bin/nph-data_query?bibcode=2008arXiv0804.4197C&link_type=ABSTRACT`. 24 pages, submitted to the Astrophysical Journal.

S Jin and Z Xin. The relaxation schemes for systems of conservation laws in arbitrary space dimensions. *Communications on Pure and Applied Mathematics*, Jan 1995. URL `http://www3.interscience.wiley.com/journal/113401027/abstract`.

S Kida. Asymptotic properties of burgers turbulence. *Journal of Fluid Mechanics*, 93:337, Jul 1979. doi: 10.1017/S0022112079001932. URL `http://adsabs.harvard.edu/cgi-bin/nph-data_query?bibcode=1979JFM....93..337K&link_type=ABSTRACT`.

Mark R Krumholz and Jonathan C Tan. Slow star formation in dense gas: Evidence and implications. *The Astrophysical Journal*, 654:304, Jan 2007. doi: 10.1086/509101. URL `http://adsabs.harvard.edu/cgi-bin/nph-data_query?bibcode=2007ApJ...654..304K&link_type=ABSTRACT`. (c) 2007: The American Astronomical Society.

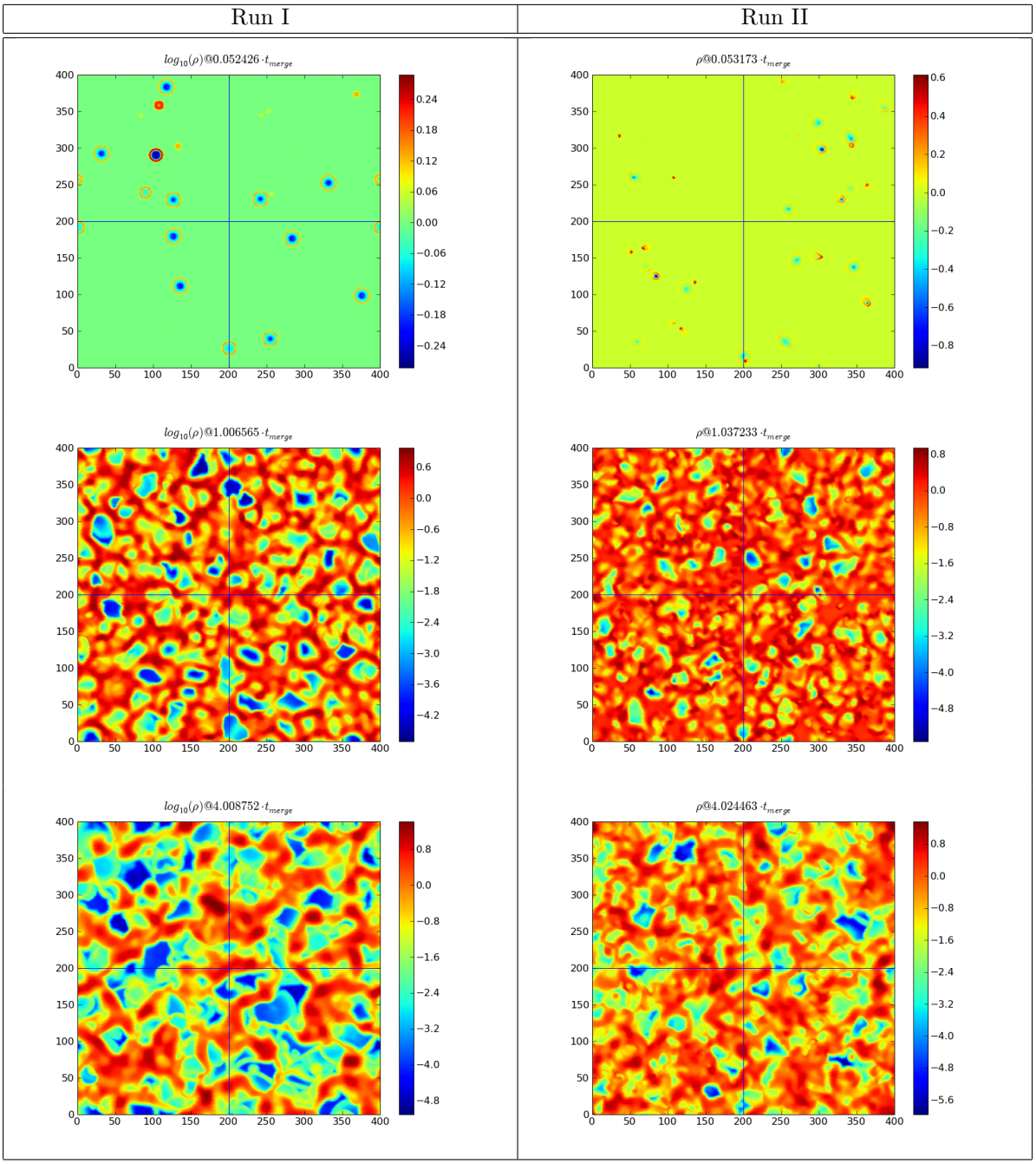

Fig. 2.— Slices of log density ($log_{10}(\rho)$) shortly after initialization ($t \approx 0$), at the merging time ($t \approx t_{merge}$) and at saturation ($t \gg t_{merge}$) for runs I and III.

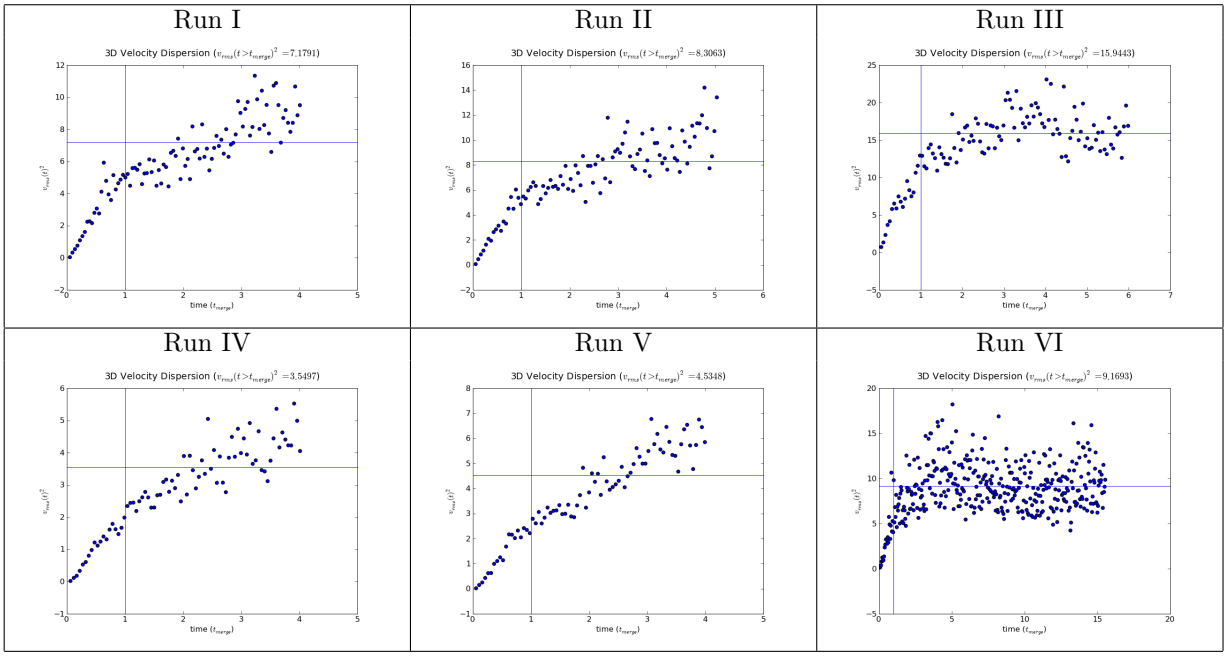

Fig. 3.— 3D velocity dispersion (v_{rms}) for all runs.

Mordecai-Mark Mac Low. The energy dissipation rate of supersonic, magnetohydrodynamic turbulence in molecular clouds. *The Astrophysical Journal*, 524:169, Oct 1999. doi: 10.1086/307784. URL `http://adsabs.harvard.edu/cgi-bin/nph-data_query?bibcode=1999ApJ...524..169M&link_type=ABSTRACT`.

Christopher D Matzner. Protostellar outflow-driven turbulence. *arXiv*, astro-ph, Jan 2007. URL `http://arxiv.org/abs/astro-ph/0701022v1`. 15 pages, 3 figures, submitted to ApJ.

Christopher D Matzner and Christopher F McKee. Bipolar molecular outflows driven by hydromagnetic protostellar winds. *arXiv*, astro-ph, Sep 1999. URL `http://arxiv.org/abs/astro-ph/9909479v1`. 4 pages, 1 figure, submitted to ApJL.

Christopher F McKee and Eve C Ostriker. Theory of star formation. *Annual Review of Astronomy & Astrophysics*, 45:565, Sep 2007. doi: 10.1146/annurev.astro.45.051806.110602. URL `http://adsabs.harvard.edu/cgi-bin/nph-data_query?bibcode=2007ARA%2526A..45..565M&link_type=ABSTRACT`.

Fumitaka Nakamura and Zhi-Yun Li. Protostellar turbulence in cluster forming regions of molecular clouds. *Triggered Star Formation in a Turbulent ISM*, 237: 306, Jan 2007. doi: 10.1017/S1743921307001640. URL `http://adsabs.harvard.edu/cgi-bin/nph-data_query?bibcode=2007IAUS..237..306N&link_type=ABSTRACT`.

Ue-Li Pen, Phil Arras, and ShingKwong Wong. A free, fast, simple, and efficient total variation diminishing magnetohydrodynamic code. *The Astrophysical Journal Supplement Series*, 149:447, Dec 2003. doi: 10.1086/378771. URL `http://adsabs.harvard.edu/cgi-bin/nph-data_query?bibcode=2003ApJS..149..447P&link_type=ABSTRACT`. (c) 2003: The American Astronomical Society.

Alice C Quillen, Stephen L Thorndike, Andy Cunningham, Adam Frank, Robert A Gutermuth, Eric G Blackman, Judith L Pipher, and Naomi Ridge. Turbulence driven by outflow-blown cavities in the molecular cloud of ngc 1333. *The Astrophysical Journal*, 632:941, Oct 2005. doi: 10.1086/444410. URL `http://adsabs.harvard.edu/cgi-bin/nph-data_query?bibcode=2005ApJ...632..941Q&link_type=ABSTRACT`. (c) 2005: The American Astronomical Society.

James M Stone, Eve C Ostriker, and Charles F Gammie. Dissipation in compressible magnetohydrodynamic turbulence. *The Astrophysical Journal*, 508:L99, Nov 1998. doi: 10.1086/311718. URL `http://adsabs.harvard.edu/cgi-bin/nph-data_query?bibcode=1998ApJ...508L..99S&link_type=ABSTRACT`. (c) 1998: The American Astronomical Society.

B Zuckerman and P Palmer. Radio radiation from interstellar molecules. *In: Annual review of astronomy and astrophysics. Volume 12. (A75-13476 03-90) Palo Alto*, 12: 279, Jan 1974. doi: 10.1146/annurev.aa.12.090174.001431. URL `http://adsabs.harvard.edu/cgi-bin/nph-data_query?bibcode=1974ARA%2526A..12..279Z&link_type=ABSTRACT`. A&AA ID. AAA012.131.074.

This 2-column preprint was prepared with the AAS LaTeX macros v5.2.